Evanescent-imaging-ellipsometry-based microarray reader

Srivatsa Venkatasubbarao
Intelligent Optical Systems
2520 West 237 Street
Torrance, California 90505
E-mail: srao@intopsys.com

Neil Beaudry
Yanming Zhao
Russell Chipman
University of Arizona
College of Optical Sciences
Meinel Building, 1630 East University Boulevard
Tucson, Arizona 85721

Abstract. We describe the development of a label-less ellipsometric imaging microarray reader. The ability of the ellipsometric microarray reader to measure binding of sample to microarray surface is verified using oligonucleotide complementary DNA (cDNA) microarrays. Polarized light illuminates the microarray surface through a glass substrate at an angle beyond the critical angle and changes in the polarization of totally internally reflected light resulting from binding events on the microarray surface are measured. This polarization change is used to measure the thickness of biomolecules bound to the microarray. A prototype ellipsometric imaging microarray reader is constructed and calibrated, and the performance is evaluated with cDNA microarrays. The microarray reader measures changes in refractive index changes as small as 0.0024 and thickness changes as small as 0.28 nm. The optimization of angle of incidence and substrate refractive index necessary to achieve high sensitivity is also described. This ellipsometric technique offers an attractive alternative to fluorescence-microarray readers in some genomic, proteomic, diagnostic, and sensing applications. [DOI: 10.1117/1.2166407]

Keywords: microarray; ellipsometry; label-less; fluorescence; diagnostics.

Paper 05100R received Apr. 19, 2005; revised manuscript received Sep. 23, 2005; accepted for publication Oct. 24, 2005; published online Jan. 31, 2006. This paper is a revision of a paper presented at the SPIE conference on Advanced Environmental, Chemical, and Biological Sensing Technologies II, Oct. 2004, Philadelphia, Pennsylvania. The paper presented there appears (unrefereed) in SPIE Proceedings Vol. 5586.

1 Introduction

Microarrays are widely used in genomic, proteomic, and diagnostic applications.[1] A microarray consists of specific biomolecules (oligonucleotide sequences, polymerase chain reaction products, proteins, etc.) immobilized as spots on a substrate surface. The microarray is then reacted with a sample containing analytes that specifically bind to immobilized biomolecules. Typically, the analytes are labeled with fluorescent dye(s) and the intensity of the bound fluorescent dye is read on a fluorescent microarray reader. The fluorescence intensity is related to the concentration of analytes bound.

Fluorescence-based microarray reading methods offer high sensitivity. The ability to use multiple fluorescent dyes that fluoresce at different wavelengths offers the attractive choice, where control and samples are to be tested in a single measurement. One of the drawbacks in using fluorescent labels arises from the additional steps that are involved in the attachment of labels to analytes. Other drawbacks are the requirement for additional steps of purification of the fluorescent labeled analytes and the photostability of fluorescent dyes. Finally, the attachment of a label to the analyte can alter its binding characteristics and may not provide a realistic picture of its biological activity. Therefore, alternative label-less methods to read microarrays are in development.[2]

This paper describes an approach to microarray readout that does not require any labels. Utilizing evanescent imaging ellipsometry, this method offers a highly sensitive alternative to fluorescent microarray readers. The following sections describe the theoretical principles of the imaging ellipsometric method, the construction of the optical detection unit, and the fabrication of microarrays for testing and the characterization of microarray readers.

2 Ellipsometric Microarray Reader Optical System

Figure 1 shows a schematic diagram of the imaging ellipsometric microarray reader that is based on a patent by Kempen.[3] The light source is a collimated green 520-nm LED. A polarizer and a quarter-wave linear retarder in rotary stages generate polarized light with adjustable orientation and ellipticity. This light enters a right-angle prism at normal incidence. The microarray is fabricated on a poly-l-lysine-coated BK7 glass slide. The microarray is mounted horizontally and the bottom surface of the microarray is affixed to the hypotenuse of the prism with index-matching fluid, as shown

Address all correspondence to Neil Beaudry, Optical Sciences Center, University of Arizona, 1630 East University Boulevard, Tucson, AZ 85721. Tel: 520–621–8253. Fax: 520–621–3389. E-mail: beaudry@u.arizona.edu

1083-3668/2006/11(1)/014028/9/$22.00 © 2006 SPIE

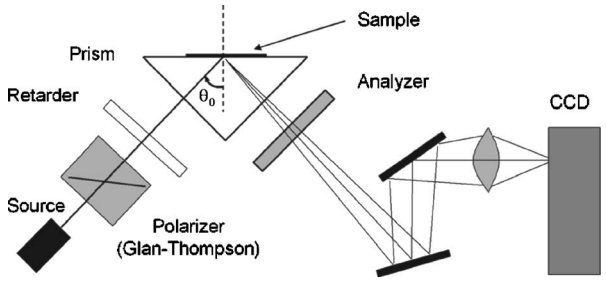

Fig. 1 Principle of evanescent imaging ellipsometric microarray reader. Polarized light illuminates the microarray surface (sample) and is totally internally reflected. The retardance and diattenuation of the microarray spots changes the polarization of the reflected beam. An analyzer nearly extinguishes the beam and the resulting intensity image is related to the thickness and refractive index of the microarray surface.

in Fig. 2. In this configuration, the incident angle on the microarray, $\theta_0=45$ deg, is larger than the critical angle of 41.2 deg.

The polarization state change at the microarray interface is primarily due to the retardance associated with total internal reflection (TIR) at a dielectric interface with additional modification due to interaction with the microarray spots. The total internally reflected light then exits the prism at normal incidence. The polarizer and retarder's orientations are adjusted such that the light reflected from the BK7 interface is linearly polarized at 135 deg. An analyzer (linear polarizer) is oriented at a 45-deg orientation to extinguish the TIR beam.

The binding of analytes to the microarray spots, cause thickness changes $t(\mathbf{x})$ and changes in complex refractive index $n(\mathbf{x})-i\kappa(\mathbf{x})$, across the surface of the microarray sample. The vector $\mathbf{x}$ is position on the microarray. These changes cause an additional alteration to the polarization state of the beam reflected from the TIR interface, inducing a small leakage of light at the polarizer.

Two folding mirrors return the beam to a horizontal axis. The light leaked through the analyzer constitutes the signal. A telephoto camera lens set at $f/20$ images the microarray onto a scientific grade 10-bit CCD camera (Optronics, MagnaFire). A photograph of the imaging ellipsometric microarray reader prototype is shown in Fig. 3. This beam has a limiting resolution of $1.22\lambda f/\#=12.6$ μm. The CCD pixel size also limits the resolution to about 12 μm. Despite the tilted image plane, the images were well resolved over a 1-cm field of view.

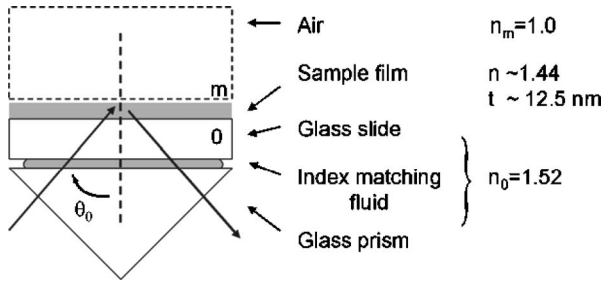

Fig. 2 Configuration through the prism with typical refractive indices.

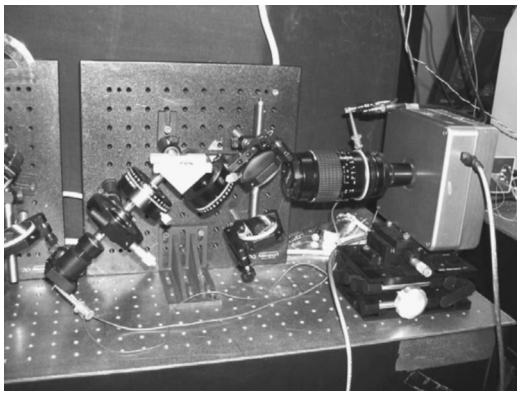

Fig. 3 Evanescent imaging ellipsometric microarray reader prototype. Sample glass slide is mounted above right angle prism (white) with index-matching fluid.

3 Principle of Operation

The ellipsometric microarray reader measures the change in the polarization state of the light reflected from the microarray surface to determine the concentration of bound analytes to microarray spots. This change is modeled using the equations of optical thin films and ellipsometry.[4–6]

At the microarray interface, the light beam undergoes TIR from the hypotenuse surface of a glass prism in contact with a microarray sample.[7,8] The reflection causes separate changes in the amplitudes and phases of the s and p components of the incident light field, which are characterized by two complex amplitude reflection coefficients r_s and r_p. For a BK-7 glass slide without microarray spots, r_s and r_p are the Fresnel reflection coefficients. For a glass slide containing layers of biomolecules, r_s and r_p are calculated by treating the biomolecules as a thin film coating. The retardance δ is defined as the relative change in phase between the p and s components of the light field and is given by

$$\delta=|\arg(r_p)-\arg(r_s)|. \tag{1}$$

The retardance and the changes in amplitude between p and s components, $\tan(\Psi)$, are characterized in ellipsometry by

$$\tan(\Psi)\exp(i\delta)=\frac{r_p}{r_s}. \tag{2}$$

The change in the amplitudes of r_s and r_p, which characterize the reflection amplitude differences for different polarization states is also characterized by the parameter diattenuation D defined as

$$D=\cos(2\Psi)=\frac{|r_s|^2-|r_p|^2}{|r_s|^2+|r_p|^2}, \tag{3}$$

a measure of partial polarization. Diattenuation varies from 0, when all polarization states have equal reflectance (such as TIR), to 1 for an ideal polarizer. When a light field undergoes TIR in nonabsorbing materials, only retardance occurs since $|r_s|=|r_p|=1$ and $D=0$. In this configuration, changes to δ arise from both variations in thickness and refractive index. When the biomolecules have absorption, a nonzero diattenuation occurs.

To obtain a linearly polarized beam at 45 deg following TIR, the polarizer and the quarter-wave plate azimuthal are selected such that the incident amplitudes of the p and s components are equal with a difference in phase opposite to the TIR retardance. As shown later, this beam should have Jones vector

$$\mathbf{E}_0 = \frac{1}{2}\begin{pmatrix} 1 \\ e^{i\delta_0} \end{pmatrix}. \tag{4}$$

Then the internally reflected beam has the Jones vector

$$\mathbf{E}_1 = \frac{1}{\sqrt{2}}\begin{pmatrix} 1 \\ 1 \end{pmatrix}. \tag{5}$$

The retardance and diattenuation of the interface are represented by Jones matrix $\mathbf{J}_s$,

$$\mathbf{J}_s = \begin{pmatrix} 1 & 0 \\ 0 & e^{i\delta} \end{pmatrix} \times \begin{pmatrix} |r_s| & 0 \\ 0 & |r_p| \end{pmatrix} = \begin{pmatrix} |r_s| & 0 \\ 0 & |r_p|e^{i\delta} \end{pmatrix}. \tag{6}$$

The reflected beam is almost completely blocked by an analyzer, a linear polarizer oriented at 135 deg with a Jones matrix

$$\frac{1}{2}\begin{pmatrix} 1 & -1 \\ -1 & 1 \end{pmatrix}. \tag{7}$$

A lens relays the light to a CCD array. For a bare glass slide, the reflected beam is completely extinguished by the analyzer.

$$\frac{1}{2}\begin{pmatrix} 1 & -1 \\ -1 & 1 \end{pmatrix} \times \mathbf{E}_1 = \begin{pmatrix} 0 \\ 0 \end{pmatrix}. \tag{8}$$

The retardance and diattenuation introduced by reflection from the spots on microarray surface cause the totally internally reflected beam to become elliptically rather than linearly polarized with Jones vector

$$\begin{pmatrix} 1 & 0 \\ 0 & e^{i\delta} \end{pmatrix} \times \begin{pmatrix} |r_s| & 0 \\ 0 & |r_p| \end{pmatrix} \times \mathbf{E}_0 = \frac{1}{2}\begin{pmatrix} |r_s| \\ |r_p| \exp(i\delta - \delta_0) \end{pmatrix}. \tag{9}$$

The diattenuation and retardance of the microarray spots prevents the light from being completely extinguished by the 135-deg analyzer because the Jones vector transmitted through the 135-deg polarizer is

$$\frac{1}{2}\begin{pmatrix} 1 & -1 \\ -1 & 1 \end{pmatrix} \times \frac{1}{2}\begin{pmatrix} |r_s| \\ |r_p| \exp(i\delta - \delta_0) \end{pmatrix} = \frac{|r_s| - |r_p| \exp(i\delta - \delta_0)}{2\sqrt{2}} \frac{1}{\sqrt{2}}\begin{pmatrix} 1 \\ -1 \end{pmatrix}. \tag{10}$$

Thus, retardance changes cause elliptically polarized light. Diattenuation causes the axis of the polarization to rotate from 135 deg. These changes depend on $t(\mathbf{x}), n(\mathbf{x})$, and $\kappa(\mathbf{x})$. The intensity of the microarray image becomes

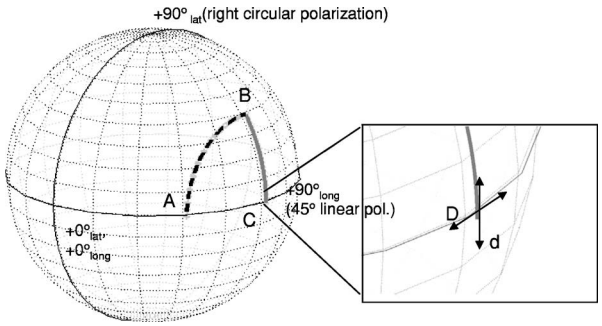

Fig. 4 Evolution of the light polarization state on the Poincaré sphere. The state after the first polarizer A is rotated to B by the quarter-wave plate oriented at 45 deg. TIR brings the state to C. The zoomed in area shows how diattenuation changes the polarization orientation and retardance δ the polarization ellipticity.

$$I_{\text{out}} = \left| \frac{|r_s| - |r_p|e^{i\delta}}{2\sqrt{2}} \right|^2 = \frac{|r_s|^2 + |r_p|^2 - 2|r_s||r_p| \cos(\delta - \delta_0)}{8} = \frac{(|r_s| - |r_p|)^2}{8} + \frac{1}{2}|r_s||r_p| \sin^2\left(\frac{\delta - \delta_0}{2}\right), \tag{11}$$

where the spatial dependence is suppressed.

For film thicknesses much smaller than the optical wavelength, the retardance change is small, $\delta - \delta_0 \ll \pi$ leading to the approximate result

$$\sin^2\left(\frac{\delta - \delta_0}{2}\right) \approx \left(\frac{\delta - \delta_0}{2}\right)^2. \tag{12}$$

Similarly, since $|r_s| \approx 1$ and $|r_p| \approx 1$, the diattenuation is small and can be approximated as

$$D = \frac{|r_s|^2 - |r_p|^2}{|r_s|^2 + |r_p|^2} \approx |r_s| - |r_p|. \tag{13}$$

Applying these approximations, the image intensity becomes

$$I \approx \frac{D^2}{8} + \frac{1}{2}\sin^2\left(\frac{\delta}{2}\right) \approx \frac{D^2 + (\delta - \delta_0)^2}{8}. \tag{14}$$

In summary, spatial variations in δ and D that occur due to the biomolecules on the microarray surface result in a nonuniform intensity distribution described by Eq. (14), which is measured by the ellipsometric microarray reader's CCD. Since the variations of $\delta(\mathbf{x})$ and $D(\mathbf{x})$ in the image are associated with the spatial variations $t(\mathbf{x})$, $n(\mathbf{x})$, and $\kappa(\mathbf{x})$ of the sample film, the image intensity provides information about these optical parameters of the sample film.

The Poincaré sphere in Fig. 4 helps explain the evolution of the light state through the polarizer, quarter wave retarder, TIR, and the small influence of film diattenuation and retardance. The objective of the setup is to end at C, 45-deg linearly polarized light. Light exits the polarizer at a position A and is rotated to B by the quarter-wave retarder oriented at 45 deg. TIR from the bare surface, a retarder at 0 deg, brings the state to C, linearly polarized at 45 deg, which will be

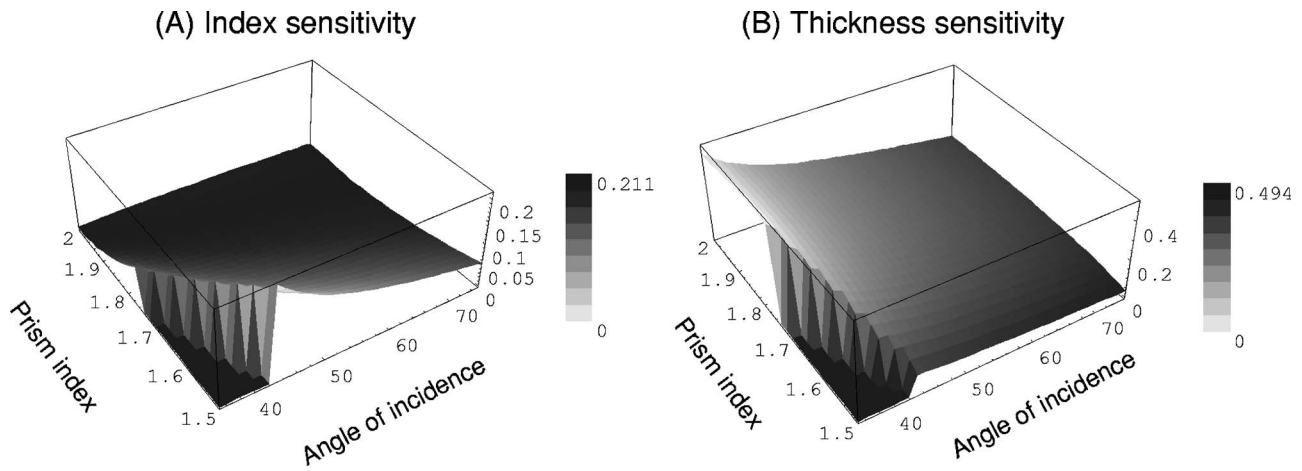

Fig. 5 (a) Sensitivity to film refractive index variation for dielectric film expressed in units of degrees of retardance per 0.01 of refractive index change and (b) layer thickness sensitivity in degree per nanometer. Area in the lower left-hand corner indicates the region below the critical angle with TIR failure.

extinguished by the final oriented analyzer. The polarizer azimuth is set at $\alpha=(\pi/2-\delta_0)/2$, where δ_0 is the retardance introduced by TIR.

Any change in retardance introduced by the microarray causes the polarization state to move along the longitude of the Poincaré sphere. Diattenuation caused by the microarray moves the polarization state along the equator. Both cause leakage at the final analyzer. Additionally, an adjustment of the initial polarizer azimuth can differentiate between the diattenuation and retardance.

For our prototype ellipsometric reader, the BK7 prism refractive index is $n_0=1.52$, the angle of incidence is $\theta_0=45$ deg, and the microarray surface is immersed in air $n_m=1.0$. A typical biomolecular layer has an index of refraction in a range $1.44<n<1.48$ and a thickness of approximately $t=12.5$ nm (Refs. 2, 9, and 10). For the nucleotide sequence of about 30 nucleic acids we estimate the index of refraction to be $n=1.44$. A thin film calculation[6] using these parameters demonstrates that a biomolecular layer introduces a retardance change, δ, from the bare interface of

$$\delta(1.44, 12.5\ \text{nm}) = 0.02277\ \text{rad} = 1.3048\ \text{deg}, \qquad (15)$$

which is readily measured by this technique.

The sensitivity to changes in refractive index and thickness is found by differentiating $\delta(n,t)$ with respect to index

$$\left|\frac{\mathrm{d}[\delta(n,t)]}{\mathrm{d}n}\right| \approx |\delta(1.445, 12.5\ \text{nm}) - \delta(1.435, 12.5\ \text{nm})| = 0.1621\ \text{deg}/0.01, \qquad (16)$$

and thickness

$$\left|\frac{\mathrm{d}[\delta(n,t)]}{\mathrm{d}n}\right| \approx |\delta(1.44, 12.0\ \text{nm}) - \delta(1.44, 13.0\ \text{nm})| = 0.1119\ \text{deg/nm}. \qquad (17)$$

The refractive index sensitivity $|\mathrm{d}[\delta]/\mathrm{d}n|$ and the layer thickness sensitivity $|\mathrm{d}[\delta]/\mathrm{d}t|$ establish the requirements for determining small thickness and index variation. These requirements include the purity of the incident polarization state, the extinction coefficient of the polarizers, and any intrinsic depolarization caused by the biomolecule spots.

The sensitivity can be improved by optimizing the prism refractive index and incident angle. Figure 5 shows the refractive index sensitivity $|\mathrm{d}(\delta)/\mathrm{d}n|$ and the layer thickness sensitivity $|\mathrm{d}(\delta)/\mathrm{d}t|$ for the typical biomolecular layer ($n=1.44$ and $t=12.5$ nm) as functions of substrate refractive index n_0 and angle of incidence θ_0.

An examination of Fig. 5 indicates the following:

1. A low angle of incidence is preferred for maximizing both $|\mathrm{d}(\delta)/\mathrm{d}n|$ and $|\mathrm{d}(\delta)/\mathrm{d}t|$.

2. A low prism index is preferred for maximizing $|\mathrm{d}(\delta)/\mathrm{d}n|$. A high prism index is preferred for maximizing $|\mathrm{d}(\delta)/\mathrm{d}t|$. Therefore, this ellipsometer configuration can be optimized for either refractive index sensitivity or thickness sensitivity, but not both simultaneously.

3. Thickness sensitivity is easier to maximize than index sensitivity. This low-refractive-index sensitivity occurs because the film is extremely thin compared to a wavelength of light.

4 Measurements and Results

4.1 *Fabrication of Microarrays*

Three OMM16K mouse complementary DNA (cDNA) arrays are used to test the imaging ellipsometric microarray reader. The microarrays contain 70-mer oligonucleotides deposited as 125-μm-diam spots printed on poly-l-lysine-coated slides in 32 subarrays of 24 columns and 23 rows each for a total of 17,664 spots using Telechem Stealth SMP3 pins in 32 pin configuration. The spots are separated by a center- to-center distance of 175 μm. The array size is $17,984\times35,968$ μm. Cy3-labeled arrays were tested to make a direct comparison of imaging ellipsometer measurements to microarray scanners that utilize Cy3 fluorescent labels. The array description and gene list can be found in Ref. 11.

Figure 6 outlines the steps to hybridize cDNA to microarray. Total RNA was prepared using Qiagen RNeasy Midi Kit. The messenger RNA (mRNA) was prepared from total RNA

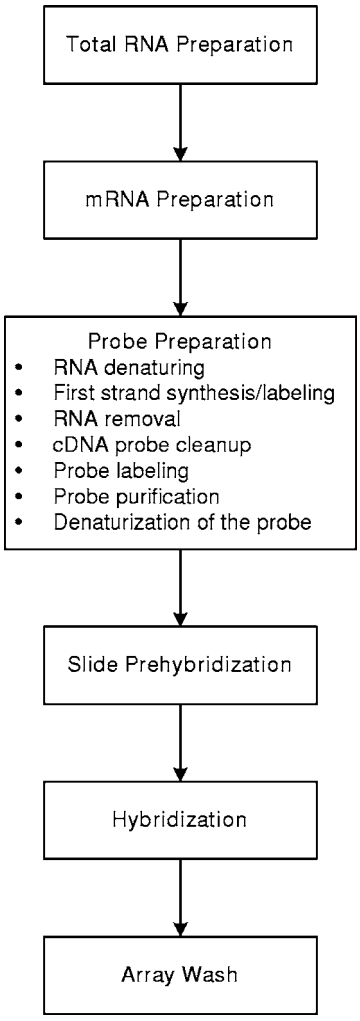

Fig. 6 Microarray fabrication protocol. To test the ellipsometric microarray reader, the probe labeling and purification steps were not performed.

using Oligotex columns from Qiagen. 25 μg of total RNA was used for each labeling reaction. Prior to labeling, total RNA was concentrated to about 3.3 $\mu g/\mu l$ using ethanol/isopropanol precipitation (1 vol. RNA+2 vol. ethanol:isopropanol 1:1). A 10-min precipitation at room temperature was followed by a 10-min spin at 14,000 rpm in a microfuge to recover the nucleic acids.

The RNA was denatured and primers were annealed by incubating 15 μL of resuspended RNA, 4 μL of oligo dT (1 $\mu g/\mu l$) and 1 μL random hexamers (5 $\mu g/\mu l$) for 5 min at 68°C. The first strand synthesis and labeling was performed by adding 8 μL 5× first strand buffer, 4 μL 0.1 M DTT, 0.6 μL 33.3 mM each dACG, 0.32 μL 25 mMdTTP, 4 μL 2 mM aa-dUTP, 1 μL RNAse to 20 μL of denatured RNA. Do microliters of Superscript-RT (Gibco) was added to this mixture and incubated at 42°C for 2 h. This was followed by heating the mixture to 94°C for 2 to 3 min.

The RNA was removed by adding 5 μL 0.5 M EDTA and 10 μL 1 M NaOH and heating for 20 min at 60 to 65°C. Then 6 μL 1 M HCl and 2 μL 1 M Tris pH 7.5 was added to neutralize NaOH. The cDNA probe was cleaned using CyScribe GFX purification kit (Amersham Biosciences, catalog #27-9606-01).

Cy3-NHS was disordered in DMSO three concentration of 5 $\mu g/\mu l$. Then 2 μL of this dye was added to each cDNA probe and incubated at room temperature for 60 to 90 min. After incubation, the reaction was halted by adding 4 μL 2 M ethanolamine at room temperature for 5 min. The labeled probe was purified by Cyscribe GFX purification kit. The purified dye labeled probe was denatured by mixing 3 μL probe with 0.5 μL 20×SSPE, 1.5 μL poly dA (5 $\mu g/\mu l$) and 8 μL hybridization buffer. The mixture was heated to 90°C for 2 min.

Next 13 μL of prehybridization buffer was added on the microarray slide and the microarray was covered with a 22-×22-mm coverslip and placed in the hybridization chamber for 1 h at 50°C. The prehybridization buffer was rinsed with water, 70% ethanol, and 100% ethanol and air dried. These microarrays were used for hybridization and testing.

The 13 μL of dye-labeled probes are added on top of the prehybridized microarray slides. The slide was covered with a 22-×22-mm cover slip and hybridized for 18 h in a hybridization chamber. These hybridize microarrays were tested by fluorescent microarray scanner and imaging ellipsometer.

4.2 *Measurement Procedure*

The hypotenuse surface of the prism is cleaned using standard optical cleaning methods. A drop of refractive index matching fluid ($n=1.52$) is placed on one edge of the hypotenuse surface and the rear surface of the glass slide is slowly attached to the hypotenuse of the prism allowing the index matching fluid to spread between the prism and the glass slide surfaces, sealing the gap. Caution is taken to avoid air bubbles trapped in the imaging area, which cause bright spots on the ellipsometric image. An image is formed of the microarray on the CCD and the polarization elements in the ellipsometer are adjusted to achieve the best null possible in the area surrounding the microarray spots. The lens is stopped down to $f/16$ to increase the depth of focus to accommodate the tilted object plane.

The Cy3-labeled probes are used to compare the results from imaging ellipsometry experiments to those from a fluorescence microarray reader (Axon Instruments). The fluorescent measurement of the Cy3-hybridized microarray is shown in Fig. 7(a). The spots are clearly visible and the measurements show bright spots with a clear dark background. Figure 7(b) shows the ellipsometric image of a similar microarray using the prototype ellipsometric microarray reader. Note that the sensitivity analysis already given demonstrated that the change in retardance caused by the microarray spots is very small. Therefore, to achieve the necessary sensitivity, the image exposure time was set to about 10 s to increase the retardance sensitivity of the instrument resulting in the camera the dynamic range being significantly smaller than the total contrast ratio of the ellipsometer. The extinction ratio of the ellipsometer was measured to be about 3000:1, and we believe this is limited by retarder uniformity and scattering within the prism.

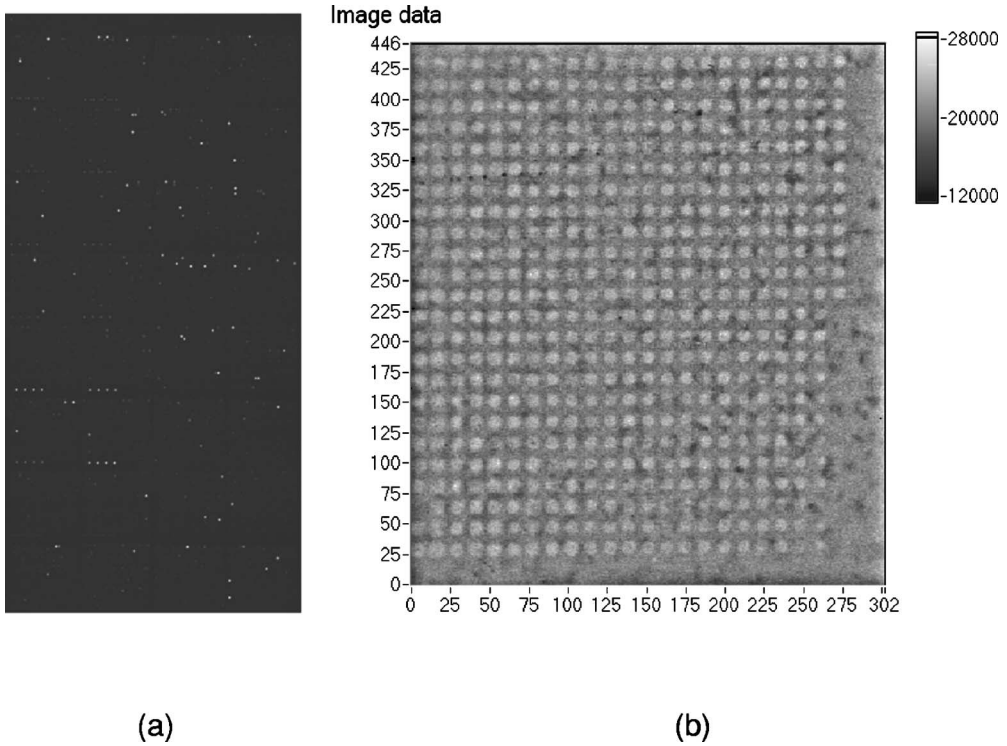

Fig. 7 (a) Cy3-hybridized microarray measured on fluorescent microarray reader from Axon Instruments and (b) DNA microarray image using benchtop ellipsometric microarray reader.

4.3 *Calibration Procedure*

The microarray reader is calibrated using a high-precision imaging Mueller matrix polarimeter (IMMP), located at the Polarization Laboratory of the Optical Science Center, University of Arizona. Figure 8 shows a schematic diagram of the IMMP system. A detailed description of this system can be found in the literature.[7,12–14] Mueller matrix images are then reduced to retardance and diattenuation maps using a polar decomposition algorithm.[15]

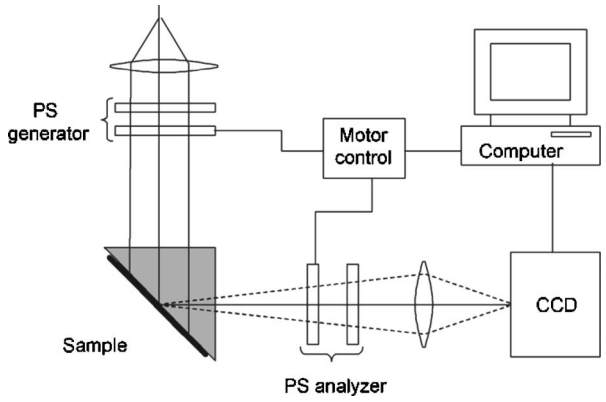

Fig. 8 Mueller matrix imaging polarimeter configured to measure microarray samples. Samples had to be mounted vertically. The resulting Mueller matrix and retardance measurements were used to calibrate the imaging ellipsometric microarray reader. The polarization state (PS) generator and the PS analyzer both contain fixed polarizers and rotating retarders (elements closer to sample).

Calibration is performed by first using the ellipsometer to acquire an image of a microarray sample. A cross section of the image is extracted and the average of the intensity variations I induced by the microarray spots is determined. Next the IMMP system is used to measure the retardance caused by TIR in the glass prism and the retardance change δ induced by the microarray spots. The intensity variation of the ellipsometer image is proportional to the square of the retardance deviation, that is, $I=c \times \delta^2$. From the IMMP retardance image, the constant c in this equation is determined.

4.3.1 *Estimating the average intensity variations induced by the microarray pixels*

The microarray image is first highpass filtered in the spatial frequency domain to remove the gradual variation in the background intensity. Figure 9 is a cross section of the image along a row of spots normalized by the digital range of the detector. The average intensity variation induced by the microarray spots is measured to be 8% of digital range of the CCD detector.

4.3.2 *Estimating the retardance deviation induced by the microarray pixels*

To determine the relationship between the image intensity and microarray spot thickness, the retardance change and the diattenuation of the microarray sample and prism are independently measured by the IMMP system. The resolution of the IMMP enables the retardance and diattenuation variations to be measured to an accuracy of better than 1%. The light paths through the prism in the IMMP measurement are set to match

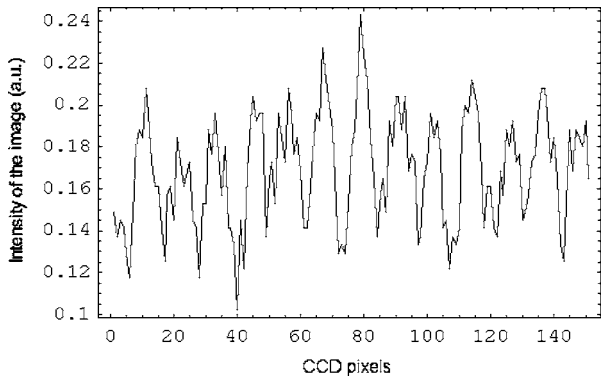

Fig. 9 Cross section of the microarray image through a row of spots acquired by the ellipsometric microarray reader.

the microarray imaging ellipsometer configuration: The wavelength is 520 nm, and the angle of incidence is 45 deg. The retardance introduced by the microarray is the dominant polarization effect contributing to the image intensity. The diattenuation introduced by the microarray sample is small ($<0.5\%$), which lies in the noise of the IMMP. Figure 10 shows a retardance image of the microarray measured by the IMMP system.

From the x and y cross sections, the mean retardance deviation introduced by a microarray spot, relative to the background (local maximum to local minimum) is measured to be

$$\delta = 0.3 \text{ deg} = 0.0052 \text{ rad}. \tag{18}$$

Assuming thickness variation at constant refractive index, then δ is related to the sample's thickness t by Eq. (17), We estimate the mean thickness change of the microarray spots as

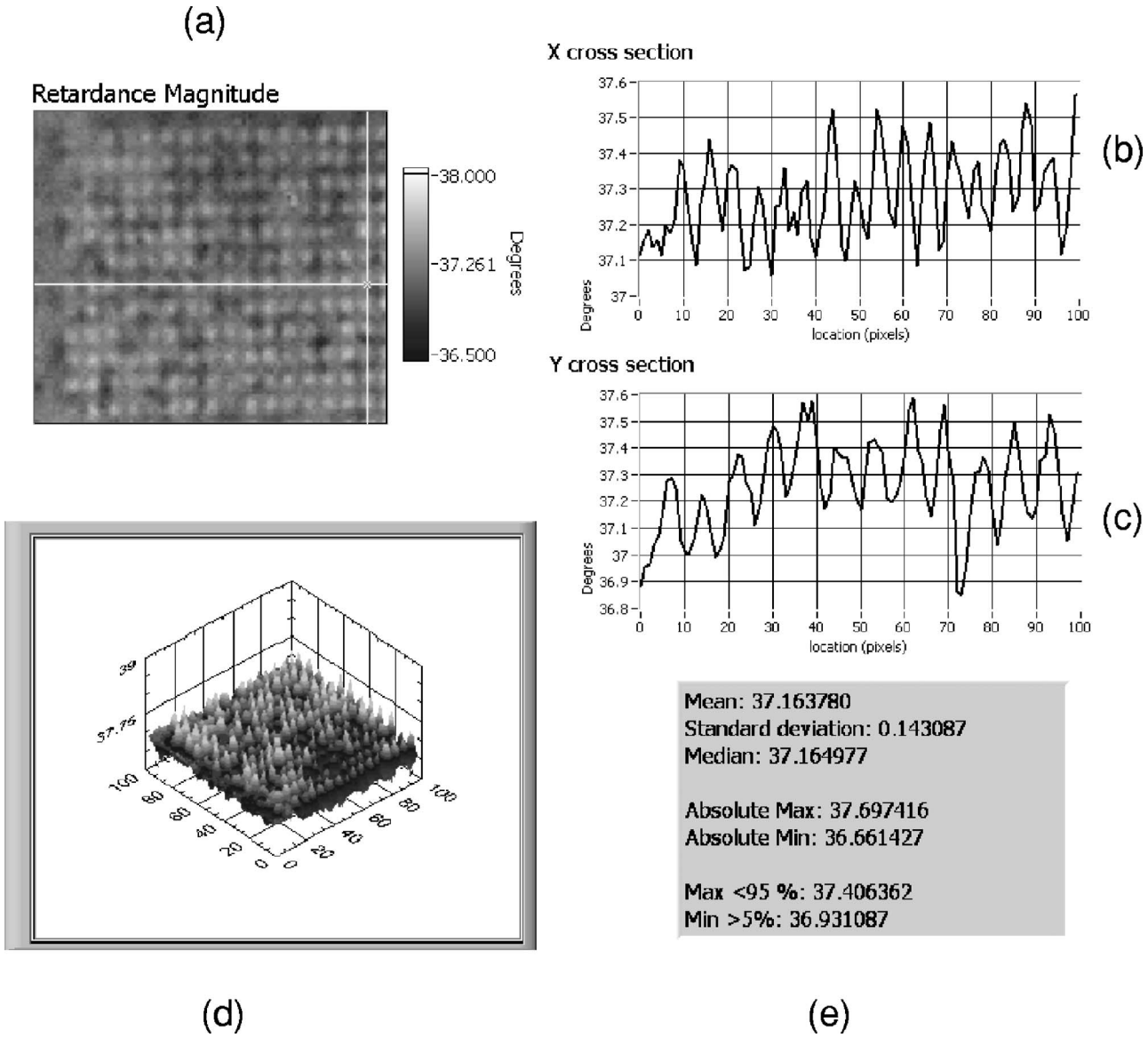

Fig. 10 (a) Retardance image of microarray measured by Mueller matrix imaging polarimeter, (b) and (c) x and y cross sections through a row and column, (d) perspective view, and (e) statistical summary. The total variation of retardance due to the microarray spots is only 1 deg.

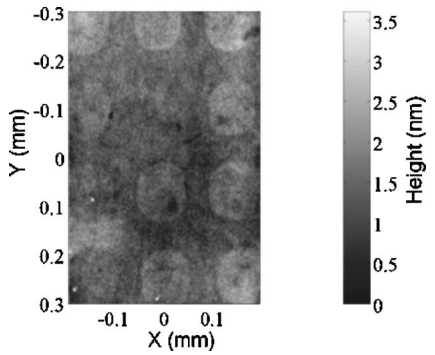

Fig. 11 Small region of the microarray (3 × 4 spots) observed with Wyko-NT2000 phase-shifting interferometer.

$$t = \frac{\delta}{|\mathrm{d}[\delta(n,t)]/\mathrm{d}t|} \approx \frac{0.3 \text{ deg}}{0.1 \text{ deg/nm}} = 3 \text{ nm}. \tag{19}$$

This thickness change is independently confirmed by a Wyko-NT2000 phase shifting interferometer measurement shown in Fig. 11 confirming that the spots are about 3 nm thick.

4.4 *System Calibration*

The retardance calibration is based on finding the constant $\boldsymbol{c}$ in the equation

$$I = c \times \delta^2. \tag{20}$$

Using

$$I = 0.08 \quad \text{and} \quad \delta = 0.3 \text{ deg} = 0.0052 \text{ rad}, \tag{21}$$

yields

$$c = 2.96 \times 10^3, \tag{22}$$

where I is the fraction of total power incident at the prism reaching the CCD.

According to the Drude approximation,[16] the retardance change δ is proportional to the thickness variation t of the extremely thin film. Thus, the calibration equation for thickness variation is

$$I = d_t \times t^2, \tag{23}$$

with

$$I = 0.08 \quad \text{and} \quad t = 3 \text{ nm}, \tag{24}$$

yields

$$d_t = 8.9 \times 10^{-3}, \tag{25}$$

where t is the value in nanometers, and d has units of nm^{-2}.

Using Equation (16), a calibration relationship between refractive index and image intensity is given by

$$I = c\left[\left|\frac{\mathrm{d}(\delta)}{\mathrm{d}n}\right| \times n_\Delta\right]^2 = d_n n_\Delta^2, \tag{26}$$

where n_Δ is the change in refractive index from a value of 1.44. Using the value $|\mathrm{d}(\delta)/\mathrm{d}n| = 0.1621/0.01 = 0.00283$ rad/0.01 from Eq. (16), and $c = 2.96 \times 10^3$ from Eq. (22) yields

$$d_n = 0.0237. \tag{27}$$

4.5 *Ellipsometer Sensitivity*

The thickness sensitivity of the ellipsometer system can be estimated by rearranging Eq. (23) and differentiating with respect to intensity.

$$\Delta t = \frac{\Delta I}{2(d_t \langle I \rangle)^{1/2}}. \tag{28}$$

The term ΔI is the uncertainty in the measured intensity, caused by noise in the camera which is estimated using

$$\text{SNR} = \frac{S \times \text{QE}}{(S \times \text{QE} + \text{dark current} + \text{read noise}^2)^{1/2}}, \tag{29}$$

where S is the number of incident photons, QE is the quantum efficiency of the camera (42% for our camera). Dark current is 40 e/pixel (over the 10-s exposure time), and the read noise is 16 e/pixel. The $S \times$ QE term in the denominator represents the effects of shot-noise on the camera intensity reading. From Fig. 9, the mean intensity signal is 16% ($I = 0.16$) of the dynamic range of the camera (16,000 e) yielding $S \times \text{QE} = 2560$ electrons, which results in a SNR=47.9, or $\Delta I = 0.0208$. Using Eq. (28) the thickness sensitivity of the ellipsometer is $\Delta t = 0.28$ nm. Using a similar analysis, the index sensitivity of the ellipsometer is $\Delta n = 0.0024$.

5 Analysis

The primary goal is to measure the binding of analytes to the biomolecules immobilized on the microarray. The change in intensity of the microarray spots shown in Fig. 7(b) demonstrate that the evanescent imaging ellipsometric microarray reader is capable of measuring a thickness change of less than 0.5 nm and a refractive index change of smaller than 0.0025. Nevertheless, the comparison with the measurement in Fig. 7(a) shows that the sensitivity to molecular binding is significantly lower than the sensitivity obtained using fluorescence measurements. The difference in sensitivity is due to the fact that the binding of analytes only causes a thickness change on the order of 1 nm. The sensitivity analysis shown in Fig. 5 demonstrates that the sensitivity of the ellipsometry system can be improved substantially by using a prism made from high-index glass (such as SF11 with an index of $n = 1.78$). However, high-index glass prisms are complicated due to difficulties with high-refractive-index-matching fluids.

6 Conclusions

The development of a label-less imaging ellipsometric microarray reader based on imaging ellipsometry was described. A prototype imaging ellipsometric system was constructed and oligonucleotide microarray samples were tested. The microarray reader is calibrated against an imaging polarimeter and a commercial interferometer. The system's thickness sensitivity is 0.28 nm and the sensitivity to refractive index changes is 0.0024.

Acknowledgments

The authors thank the National Aeronautics and Space Administration (NASA) for financial support of this work through Contract No. NNM04AA24C.

References

1. S. Venkatasubbarao, "Microarrays: current status and prospects," *Trends Biotechnol.* **22**(12), 630–637 (2004).
2. B. P. Nelson, T. E. Grimsrud, M. R. Liles, R. M. Goodman, and R. M. Corn, "Surface plasmon resonance imaging measurements of DNA and RNA hybridization adsorption onto DNA microarrays," *Anal. Chem.* **73**, 1–7 (2001).
3. L. U. Kempen, "Imaging apparatus and method," U.S. Patent No. 6594011 B1 (2003).
4. R. M. A. Azzam and N. M. Bashara, *Ellipsometry and Polarized Light*, 2nd ed., Elsevier, Amsterdam (1987).
5. P. Yeh, *Optical Waves in Layered Media*, 2nd ed., Wiley-Interscience, New York (2005).
6. H. A. Macleod, *Thin Film Optical Filters*, 3rd. ed., Institute of Physics Publishing, London (2001).
7. R. A. Chipman, "Polarimetry," in *OSA Handbook of Optics*, pp. 22.1–22.35, McGraw-Hill, New York (1995).
8. G. Jin, P. Tengvall, I. Lundström, and H. Arwin, "A biosensor concept based on imaging ellipsometry for visualization of biomolecular interactions," *Anal. Chem.* **232**(1), 69–72 (1995).
9. H. Arwin, "Ellipsometry on thin organic layers of biological interest: characterization and application," *Thin Solid Films* **377–378**, 48–56 (2000).
10. P. Tengvall, I. Lundstrom, and B. Liedberg, "Protein adsorption studies on model organic surfaces: an ellipsometric and infared spectroscopic approach," *Biomaterials* **19**, 407–422 (1998).
11. Internet website: http://keck.med.yale.edu/dnaarrays/arraydescriptions.htm#mouse.
12. J. L. Pezzaniti and R. A. Chipman, "Mueller matrix imaging polarimetry," *Opt. Eng.* **34**(6), 1558 (1995).
13. D. H. Goldstein, "Mueller matrix dual-rotating retarder polarimeter," *Appl. Opt.* **31**(31), 6676–6683 (1992).
14. R. M. A. Azzam, "A simple Fourier photo-polarimeter with rotating polarizer and analyzer for measuring Jones and Mueller matrices," *Opt. Commun.* **25**(2), 137–140 (1978).
15. J. Liu and R. M. A. Azzam, "Polarization properties of corner-cube retroreflectors: theory and experiment," *Appl. Opt.* **36**(7), 1553–1559 (1997).
16. P. Drude, "Ueber die Reflexion und Brechung ebeber Lichtwellen beim Durchgang durch eine mit Oberflächenschichten behaftete planparallel Platte" in *Wied. Ann.* **43**, 126 (1891).